Role of the $\Delta^*(1940)$ in the $\pi^+p \to K^+\Sigma^+(1385)$ and $pp \to nK^+\Sigma^+(1385)$ reactions

Ju-Jun Xie,[1,2,3,*] En Wang,[4,†] and Bing-Song Zou[3,‡]

[1] *Institute of Modern Physics, Chinese Academy of Sciences, Lanzhou 730000, China*
[2] *Research Center for Hadron and CSR Physics, Institute of Modern Physics of CAS and Lanzhou University, Lanzhou 730000, China*
[3] *State Key Laboratory of Theoretical Physics, Institute of Theoretical Physics, Chinese Academy of Sciences, Beijing 100190, China*
[4] *Departamento de Física Teórica and IFIC, Centro Mixto Universidad de Valencia-CSIC, Institutos de Investigación de Paterna, Aptd. 22085, E-46071 Valencia, Spain*

The $pp \to nK^+\Sigma^+(1385)$ reaction is a very good isospin 3/2 filter for studying Δ^{++*} resonance decaying to $K^+\Sigma^+(1385)$. Within the effective Lagrangian method, we investigate the $\Sigma(1385)$ (spin-parity $J^P = 3/2^+$) hadronic production in the $\pi^+p \to K^+\Sigma^+(1385)$ and $pp \to nK^+\Sigma^+(1385)$ reactions. For $\pi^+p \to K^+\Sigma^+(1385)$ reaction, in addition to the "background" contributions from t-channel K^{*0} exchange, u-channel $\Lambda(1115)$ and $\Sigma^0(1193)$ exchange, we also consider the contribution from the s-channel $\Delta^*(1940)$ resonance, which has significant coupling to $K\Sigma(1385)$ channel. We show that the inclusion of the $\Delta^*(1940)$ resonance leads to a fairly good description of the low energy experimental total cross section data of $\pi^+p \to K^+\Sigma^+(1385)$ reaction. Basing on the study of $\pi^+p \to K^+\Sigma^+(1385)$ reaction and with the assumption that the excitation of $\Delta^*(1940)$ resonance dominants the $pp \to nK^+\Sigma^+(1385)$ reaction, we calculate the total and differential cross sections of the $pp \to nK^+\Sigma^+(1385)$ reaction. It is shown that the new experimental data support the important role played by the $\Delta^*(1940)$ resonance with a mass in the region of 1940 MeV and a width of around 200 MeV. We also demonstrate that the invariant mass distribution and the Dalitz Plot provide direct information of the $\Sigma^+(1385)$ production, which can be tested by future experiments.

PACS numbers: 13.75.-n; 14.20.Gk; 13.30.Eg.

arXiv:1405.5586v2 [nucl-th] 19 Nov 2014

I. INTRODUCTION

Study of the spectrum of isospin 3/2 $\Delta^{++}(1232)$ excited states is one of the most important issues in hadronic physics and is attracting much attention because it is the most experimentally accessible system composed of three identical valence quarks. However, our knowledge on these resonances mainly comes from old πN experiments and is still very poor [1, 2]. In the energy region around or above 2.0 GeV, there are still many theoretical predictions of "missing Δ^* states", within the constituent quark [3] or chiral unitary [4–7] approaches, which have so far not been observed. Searching for these "missing Δ^* states" from other production processes is necessary [8, 9]. A possible new excellent source for studying these Δ^* resonance comprises the $\pi^+p \to K^+\Sigma^+(1385)$ and $pp \to nK^+\Sigma^+(1385)$ reactions, which have a special advantage since there is no contributions from isospin 1/2 nucleon resonances because of the isospin and charge conservations. In addition, those reactions require the creation of an $\bar{s}s$ quark pair. Thus, a thorough and dedicated study of the strangeness production mechanism in those reactions has the potential to gain a deeper understanding of the interaction among strange hadrons and also the nature of the Δ^* resonances.

In analogy to the $\Delta(1232)$ as first-excited state of the nucleon, the $\Sigma(1385)$ is the first-excited state of the $\Sigma(1193)$ hyperon and has a spin-parity of $3/2^+$ and isospin 1. This resonance is considered as a standard quark triplet and cataloged in the baryon decuplet, but its vicinity to the $\Lambda(1405)$ state in the mass spectrum correlates the study and the understanding of the two resonances. On the other hand, a Σ state, $\Sigma(1380)$ (spin-parity $J^P = 1/2^-$) with mass about 1380 MeV, was predicted in the framework of the diquark-diquark-antiquark picture [10–12]. This new state will make effects in the production of $\Sigma(1385)$ and then the analysis of the $\Sigma(1385)$ resonance suffers from the overlapping mass distributions and the common $\pi\Lambda(1115)$ decay mode.

There were pioneering measurements in the 1970s, the first $pp \to nK^+\Sigma^+(1385)$ cross sections in the high energy region, with beam momentum $p_{\rm lab} = 6$ GeV, were reported in Ref. [13]. Recently, this reaction was examined at 3.5 GeV beam energy by HADES Collaboration [14]. The results of angular distributions of the $\Sigma^+(1385)$ in different reference frame show that there could be contribution from an intermediate Δ^* resonance via the decay of $\Delta^{++*} \to K^+\Sigma^+(1385)$. Thus, the study of the possible role played by Δ^* resonances in the available new data from the HADES Collaboration is timely and could shed light on the complicated dynamics that governs the spectrum of these Δ^* states.

The theoretical activity has also run in parallel. Thinking of the $pp \to nK^+\Sigma^+(1385)$ reaction, the one-boson exchange model can be considered. By using this

*Electronic address: xiejujun@impcas.ac.cn
†Electronic address: En.Wang@ific.uv.es
‡Electronic address: zoubs@itp.ac.cn

frame, several theoretical calculations by considering the π exchange diagrams [13], the π and K exchange diagrams [15], and the intermediate Δ^{++} excitation [16], exist for describing the old and high energy data of Ref. [13]. These theoretical studies have traditionally been limited by the lack of knowledge on the $\Delta^*\Sigma(1385)K$ coupling strength and also the new experimental measurements from HADES [14].

In this work, we study the $\pi^+p \to K^+\Sigma^+(1385)$ and $pp \to nK^+\Sigma^+(1385)$ reactions within the effective Lagrangian method by examining the important role of the Δ^* resonances in these reactions. For the $\pi^+p \to K^+\Sigma^+(1385)$ reaction, in addition to the "background" contributions from the t-channel K^{*0} exchange, and u-channel $\Lambda(1115)$ and $\Sigma^0(1193)$ hyperon pole terms, we also study possible contributions from Δ^* resonances in the s-channel. Based on the results obtained from $\pi^+p \to K^+\Sigma^+(1385)$ reaction, we tend to study the role of Δ^* resonances in the $pp \to nK^+\Sigma^+(1385)$ reaction with the assumption that the production mechanism is due to the π^+-meson exchange with the aim of describing the new experimental data reported by HADES. Unfortunately, the information about the strong coupling of $\Delta^*K\Sigma(1385)$ is scarce [2]. Thus, it is necessary to rely on theoretical schemes, such that of Refs. [17, 18] based on a quark model (QM) for baryons. Among the possible Δ^* resonances, we have finally considered only the two-star D-wave $J^P = 3/2^-$ $\Delta^*(1940)$, which is predicted to have visible contribution [18] to the $K\Sigma(1385)$ production. Indeed, in Refs. [19–22], the contribution from a Δ^* resonance with spin-parity $3/2^-$ and mass around 2 GeV was studied in the $\gamma p \to K^+\Sigma^0(1385)$ reaction. They all found that this Δ^* resonance has a significant coupling to $K\Sigma(1385)$ channel and plays an important role in the reaction of $\gamma p \to K^+\Sigma^0(1385)$.[1] Although the $\Delta^*(1940)$ resonance is listed in the Particle Data Group (PDG) book, the evidence of its existence is poor or only fair and further work is required to verify its existence and to know its properties, accordingly, its total decay width and branching ratios are not experimentally known, either. In this respect, the HADES measurements could be used to determine some properties of this resonance.

To end this introduction, we would like to mention that in Refs. [19–22], the role played by another Δ^* resonance, $\Delta^*(2000)$ (spin-parity $J^P = 5/2^+$), in the $\gamma p \to K^+\Sigma^0(1385)$ reaction has been also studied. In these works, it is shown that the $\Delta^*(2000)$ resonance has a dominant contribution. However, it is pointed out, in Ref. [23], that the nominal mass of the $\Delta^*(2000)$ resonance does not correspond in fact to any experimental analysis but to an estimation based on the value of masses ($\sim$ 1740 and 2200 MeV) extracted from different data analysis [2]. From the results obtained in Ref. [23] we may conclude that the two distinctive resonances, $\Delta^*(\sim 1740)$ and $\Delta^*(\sim 2200)$, should be cataloged instead of $\Delta^*(2000)$. We thus will not consider the contribution from $\Delta^*(2000)$ resonance in the present work.

In the next section, we will show the formalism and ingredients in our calculation, then numerical results and discussions are presented in Sect. III. A short summary is given in the last section.

II. FORMALISM AND INGREDIENTS

The combination of effective Lagrangian approach and isobar model is an important theoretical tool in describing the various processes in the region of resonance produced. In this section, we introduce the theoretical formalism and ingredients to calculate the $\Sigma(1385)$ ($\equiv \Sigma^*$) hadronic production in $\pi^+p \to K^+\Sigma^+(1385)$ and $pp \to nK^+\Sigma^+(1385)$ reactions within the effective Lagrangian approach and isobar model.

Because we only consider the tree diagrams for the $\pi^+p \to K^+\Sigma^+(1385)$ and $pp \to nK^+\Sigma^+(1385)$ reactions, the total scattering amplitudes have not taken into account of the unitary requirements, which may be important for extracting the parameters of the baryon resonances from the analysis of the experimental data [24, 25], especially for those reactions involving many intermediate couple channels and three-particle final states [26, 27]. On the other hand, we know that it is difficult to really apply the unitary constraints in the three body cases, which need to include the complex loop diagrams [27–29], and the extracted rough parameters for the major resonances still provide useful information, hence we will leave it to further studies. Nevertheless, our model used in the present work can give a reasonable description of the experimental data in the considered energy region. Meanwhile, our calculation offers some important clues for the mechanisms of the $\pi^+p \to K^+\Sigma^+(1385)$ and $pp \to nK^+\Sigma^+(1385)$ reactions and makes a first effort to study the role of the $\Delta^*(1940)$ resonance in the relevant reactions.

A. Feynman diagrams and effective interaction Lagrangian densities

The basic tree level Feynman diagrams for the $\pi^+p \to K^+\Sigma^+(1385)$ and $pp \to nK^+\Sigma^+(1385)$ reactions are depicted in Fig. 1 and Fig. 2, respectively. For the $\pi^+p \to K^+\Sigma^+(1385)$ reaction, in addition to the "background" diagrams, such as t-channel K^{*0} exchange [Fig. 1(b)], u-channel $\Lambda(1115)$ and $\Sigma^0(1193)$ exchange [Fig. 1(c)], we also consider the s-channel $\Delta^{++*}(1940)$ ($\equiv \Delta^*$) resonance excitation process [Fig. 1(a)].

In Fig. 2, we show the tree-level Feynman diagrams for $pp \to nK^+\Sigma^+(1385)$ reaction. The diagram Fig. 2(a) and Fig. 2(c) show the direct processes, while Fig. 2(b)

[1] In Refs. [20, 21], the role played by the pentaquark state, $\Sigma^*(1380)$ (spin-parity $J^P = 1/2^-$), is also studied. But the knowledge on this state is very scarce. We thus leave the investigation on the role of this new state to a future study.

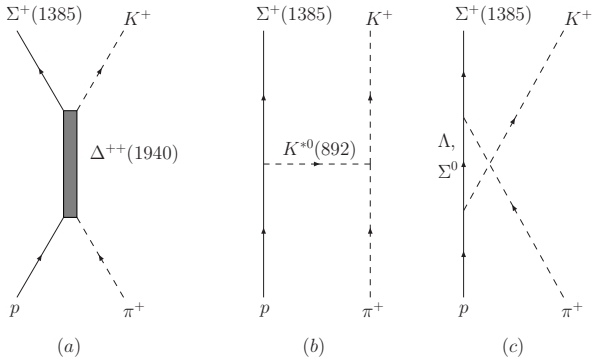

FIG. 1: Feynman diagrams for $\pi^+ p \to K^+\Sigma^+(1385)$ reaction. The contributions from s-channel $\Delta^{++}(1940)$ resonance, t-channel K^{*0} exchange, and u-channel $\Lambda(1115)$ and $\Sigma^0(1193)$ exchange are considered.

and Fig. 2(d) show the exchange processes. It is assumed that the production of the $K^+\Sigma^+(1385)$ passes mainly through the $\Delta^{+++}(1940)$, which has a significant coupling to $K\Sigma(1385)$. In this case, the t-channel K^{*0} exchange and u-channel $\Sigma^0(1193)$ exchange processes are neglected since their contributions are small, which will be discussed below.

For the $\pi^+ p \to K^+\Sigma^+(1385)$ reaction, to compute the contributions of those terms shown in Fig. 1, we use the interaction Lagrangian densities as in Refs. [19, 30, 31],

$$\mathcal{L}_{\pi N\Delta^*} = \frac{g_{\pi N\Delta^*}}{m_\pi}\bar{\Delta}^{*\mu}\gamma_5(\partial_\mu\vec{\tau}\cdot\vec{\pi})N + \text{h.c.}, \quad (1)$$

$$\mathcal{L}_{K\Sigma^*\Delta^*} = \frac{g_1}{m_K}\bar{\Sigma}^*_\mu\gamma_\alpha(\partial^\alpha K)\Delta^{*\mu} + \frac{ig_2}{m_K^2}\bar{\Sigma}^*_\mu\left(\partial^\mu\partial_\nu K\right)\Delta^{*\nu} + \text{h.c.}, \quad (2)$$

for the s-channel $\Delta^*(1940)$ processes, and

$$\mathcal{L}_{K^*N\Sigma^*} = i\frac{g_{K^*N\Sigma^*}}{2m_N}\bar{N}\gamma^\nu\gamma_5\Sigma^{*\mu}(\partial_\mu K^*_\nu - \partial_\nu K^*_\mu) + \text{h.c.}, \quad (3)$$

$$\mathcal{L}_{K^*K\pi} = g_{K^*K\pi}[\bar{K}(\partial^\mu\vec{\tau}\cdot\vec{\pi}) - (\partial^\mu\bar{K})\vec{\tau}\cdot\vec{\pi}]K^*_\mu + \text{h.c.}, \quad (4)$$

for the t-channel K^{*0} exchange process, while

$$\mathcal{L}_{KN\Sigma/\Lambda} = -ig_{KN\Sigma/\Lambda}\bar{N}\gamma_5 K\Sigma/\Lambda + \text{h.c.}, \quad (5)$$

$$\mathcal{L}_{\Sigma^*\pi\Sigma/\Lambda} = \frac{g_{\Sigma^*\pi\Sigma/\Lambda}}{m_\pi}\bar{\Sigma}^{*\mu}(\partial_\mu\vec{\tau}\cdot\vec{\pi})\Sigma/\Lambda + \text{h.c.}, \quad (6)$$

for the u-channel $\Sigma^0(1193)$ and $\Lambda(1115)$ exchange diagrams.

The above Lagrangian densities are also used to study the contributions of the terms shown in Fig. 2 for $pp \to nK^+\Sigma^+(1385)$ reaction. In addition, we also need the Lagrangian density as following for the πNN vertex,

$$\mathcal{L}_{\pi NN} = -ig_{\pi NN}\bar{N}\gamma_5\vec{\tau}\cdot\vec{\pi}N. \quad (7)$$

B. Coupling constants and form factors

Firstly, the coupling constant for πNN vertex is taken to be $g_{\pi NN} = 13.45$, while the coupling constants $g_{KN\Sigma}$, $g_{KN\Lambda}$, and $g_{K^*N\Sigma^*}$[2] are respectively taken as 2.69, -13.98, and -5.48, which are obtained from the SU(3) flavor symmetry. And these values have also been used in previous works [9, 19, 31–33].

Secondly, the coupling constants, $g_{K^*K\pi}$, $g_{\Sigma^*\pi\Sigma}$, and $g_{\Sigma^*\pi\Lambda}$, are determined from the experimentally observed partial decay widths of the $K^* \to K\pi$, $\Sigma(1385) \to \pi\Sigma$, and $\Sigma(1385) \to \pi\Lambda$, respectively. With the effective interaction Lagrangians described by Eq. (4) and Eq. (6), the partial decay widths $\Gamma_{K^*\to K\pi}$ and $\Gamma_{\Sigma(1385)\to\pi\Sigma/\Lambda}$ can be easily calculated. The coupling constants are related to the partial decay widths as,

$$\Gamma_{K^*\to K\pi} = \frac{g^2_{K^*K\pi}}{2\pi}\frac{|\overrightarrow{p}^{\text{c.m.}}_\pi|^3}{m^2_{K^*}}, \quad (8)$$

$$\Gamma_{\Sigma^*\to\pi\Sigma/\Lambda} = \frac{f_I g^2_{\Sigma^*\pi\Sigma/\Lambda}}{12\pi}\frac{|\overrightarrow{p}^{\text{c.m.}}_{\Sigma/\Lambda}|^3(E_{\Sigma/\Lambda}+m_{\Sigma/\Lambda})}{m^2_\pi M_{\Sigma^*}}, \quad (9)$$

with the isospin factor $f_I = 2$ for $\Sigma^* \to \pi\Sigma$ and $f_I = 1$ for $\Sigma^* \to \pi\Lambda$, and

$$E_{\Sigma/\Lambda} = \frac{M^2_{\Sigma^*} + m^2_{\Sigma/\Lambda} - m^2_\pi}{2M_{\Sigma^*}},$$

$$|\overrightarrow{p}^{\text{c.m.}}_{\Sigma/\Lambda}| = \sqrt{E^2_{\Sigma/\Lambda} - m^2_{\Sigma/\Lambda}},$$

$$|\overrightarrow{p}^{\text{c.m.}}_\pi| = \frac{\sqrt{[m^2_{K^*} - (m_K+m_\pi)^2][m^2_{K^*} - (m_K-m_\pi)^2]}}{2m_{K^*}}.$$

[2] In principle, there are three terms for $K^*N\Sigma^*$ vertex as used in Ref. [19] (see Eq. (6) of that reference for more details). However, there is no more information about this vertex, and it is found that the other two couplings give minor contributions to the $\gamma p \to K^+\Sigma^0(1385)$ reaction [19]. Thus, we ignore the contributions from the other two couplings.

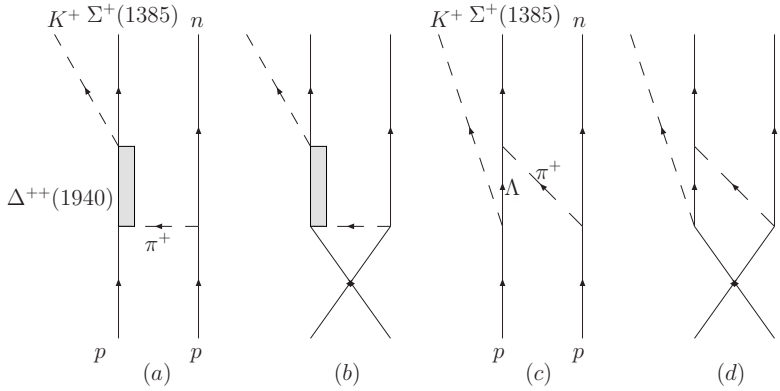

FIG. 2: Feynman diagrams for $pp \to nK^+\Sigma^+(1385)$ reaction. The diagrams (a) and (c) show the direct processes, while (b) and (d) show the exchange processes.

With mass ($M_{\Sigma^*} = 1384.57$ MeV, $m_{K^*} = 893.1$ MeV), total decay width ($\Gamma_{\Sigma^*} = 37.13$ MeV, $\Gamma_{K^*} = 49.3$ MeV), and decay branching ratios of $\Sigma(1385)$ [$\mathrm{Br}(\Sigma^* \to \pi\Sigma) = 0.117 \pm 0.015$, $\mathrm{Br}(\Sigma^* \to \pi\Lambda) = 0.87 \pm 0.015$] and K^* [$\mathrm{Br}(K^* \to K\pi) \sim 1$], we obtain these coupling constants as listed in Table I.

TABLE I: Values of the coupling constants required for the estimation of the $\pi^+p \to K^+\Sigma^+(1385)$ and $pp \to nK^+\Sigma^+(1385)$ reactions. These have been estimated from the decay branching ratios quoted in the PDG book [2], though it should be noted that these are for all final charged state.

Decay modes	Adopted branching ratios	g [a]
$\Sigma^* \to \pi\Lambda$	0.87	1.26
$\Sigma^* \to \pi\Sigma$	0.12	0.69
$K^* \to K\pi$	1.00	3.24

[a]It should be stressed that the partial decay width determine only the square of the corresponding coupling constants as shown in Eqs. (8, 9), thus their signs remain uncertain. Predictions from quark model can be used to constrain these signs. Unfortunately, quark model calculations for these vertices are still sparse. We thus choose a positive sign for these coupling constants.

Finally, the strong coupling constants $g_{\pi N\Delta^*}$ and $g_{1,2}$ for the $\Delta^*(1940)\Sigma(1385)K$ vertex are free parameters, which will be determined by fitting to the experimental data on the total cross sections of the $\pi^+p \to K^+\Sigma^+(1385)$ reaction.

In evaluating the scattering amplitudes of $\pi^+p \to K^+\Sigma^+(1385)$ and $pp \to nK^+\Sigma^+(1385)$ reactions, we need to include the form factors because the hadrons are not point like particles. We adopt here the common scheme used in many previous works,

$$f_i = \frac{\Lambda_i^4}{\Lambda_i^4 + (q_i^2 - M_i^2)^2}, \quad i = s, t, u, \tag{10}$$

$$\text{with} \quad \begin{cases} q_s^2 = s,\, q_t^2 = t,\, q_u^2 = u, \\ M_s = M_{\Delta^*}, M_t = m_{K^*}, \\ M_u = m_\Sigma, m_\Lambda, \end{cases} \tag{11}$$

where s, t and u are the Lorentz-invariant Mandelstam variables. In the present calculation, $q_s = p_1 + p_2$, $q_t = p_1 - p_3$, and $q_u = p_4 - p_1$ are the 4-momentum of intermediate $\Delta^*(1940)$ resonance in the s-channel, exchanged $K^{*0}(892)$ meson in the t-channel, and exchanged $\Sigma^0(1193)$ and $\Lambda(1115)$ in the u-channel, respectively. While p_1, p_2, p_3 and p_4 are the 4-momenta for π^+, p, K^+ and $\Sigma^+(1385)$, respectively. In principle, the cutoff Λ_s, Λ_t and Λ_u are free parameters of the model, but in practice we will constrain them to a common value between 0.6 and 1.2 GeV. By doing this, we can reduce the number of the free parameters.

C. Scattering amplitudes

The invariant scattering amplitudes that enter our model for calculation of the total cross sections for the

$$\pi^+(p_1)p(p_2, s_p) \to K^+(p_3)\Sigma^+(1385)(p_4, s_{\Sigma^*}) \tag{12}$$

are defined as

$$-iT_i = \bar{u}_\mu(p_4, s_{\Sigma^*})A_i^\mu u(p_2, s_p), \tag{13}$$

where u_μ and u are dimensionless Rarita-Schwinger and Dirac spinors, respectively, while s_{Σ^*} and s_p are the spin polarization variables for final $\Sigma^+(1385)$ and initial proton, respectively. To get the scattering amplitudes, we need also the propagators for $\Delta^*(1940)$, K^* meson, and Σ^0/Λ hyperon,

$$G_{K^*}^{\mu\nu}(q_t) = i\frac{-g^{\mu\nu} + q_t^\mu q_t^\nu/m_{K^*}^2}{t - m_{K^*}^2}, \tag{14}$$

$$G_{\Sigma/\Lambda}(q_u) = i\frac{\not{q}_u + m_{\Sigma/\Lambda}}{u - m_{\Sigma/\Lambda}^2}, \tag{15}$$

$$G_{\Delta^*}^{\mu\nu}(q_s) = i\frac{\not{q}_s + M_{\Delta^*}}{D}P^{\mu\nu}, \tag{16}$$

with

$$D = s - M^2_{\Delta^*} + iM_{\Delta^*}\Gamma_{\Delta^*}, \quad (17)$$

$$P^{\mu\nu} = -g^{\mu\nu} + \frac{1}{3}\gamma^\mu\gamma^\nu + \frac{2}{3M^2_{\Delta^*}}q_s^\mu q_s^\nu + \frac{1}{3M_{\Delta^*}}(\gamma^\mu q_s^\nu - \gamma^\nu q_s^\mu), \quad (18)$$

where M_{Δ^*} and Γ_{Δ^*} are the mass and total decay width of the $\Delta^*(1940)$ resonance, respectively. Because M_{Δ^*} and Γ_{Δ^*} have large experimental uncertainties [2], we take them as free parameters and will fit them to the total cross sections of $\pi^+p \to K^+\Sigma^+(1385)$ reaction.

Then, the reduced A_i^μ amplitudes in Eq. (13) can be easily obtained,

$$\begin{aligned} A_s^\mu &= i\frac{g_{\pi N\Delta^*}}{m_\pi D}\Big[\frac{g_1}{m_K}\not{p}_3(\not{q}_s + M_{\Delta^*})\Big(p_1^\mu - \frac{1}{3}\gamma^\mu\not{p}_1 - \\ &\frac{1}{3M_{\Delta^*}}(\gamma^\mu q_s\cdot p_1 - q_s^\mu\not{p}_1) - \frac{2}{3M^2_{\Delta^*}}q_s^\mu q_s\cdot p_1\Big) - \\ &\frac{g_2}{m_K^2}(\not{q}_s + M_{\Delta^*})p_3^\mu\Big(p_1\cdot p_3 - \frac{1}{3}\not{p}_3\not{p}_1 - \\ &\frac{1}{3M_{\Delta^*}}(\not{p}_3 q_s\cdot p_1 - q_s\cdot p_3\not{p}_1) - \\ &\frac{2}{3M^2_{\Delta^*}}q_s\cdot p_3 q_s\cdot p_1\Big)\Big]f_s, \end{aligned} \quad (19)$$

$$A_t^\mu = \frac{\sqrt{2}g_{K^*K\pi}g_{K^*N\Sigma^*}}{m_N(t-m^2_{K^*})}(\not{p}_3 p_1^\mu - \not{p}_1 p_3^\mu)f_t, \quad (20)$$

$$A_u^\mu = i\frac{g_{\Sigma^*\pi\Sigma/\Lambda}g_{KN\Sigma/\Lambda}}{m_\pi(u-m^2_{\Sigma/\Lambda})}(\not{q}_u + m_{\Sigma/\Lambda})\gamma_5 p_1^\mu f_u, \quad (21)$$

with the sub-indices s, t and u stand for the s-channel $\Delta^*(1940)$, t-channel $K^{*0}(892)$ exchange, and u-channel $\Sigma^0(1193)$ and $\Lambda(1115)$ exchange, respectively. As we can see, in the tree-level approximation, only the products, such as $g_1 g_{\pi N\Delta^*}$ ($\equiv \tilde{g}_1$) and $g_2 g_{\pi N\Delta^*}$ ($\equiv \tilde{g}_2$) enter the invariant scattering amplitudes. Because the information on these couplings are scarce, they are also determined by fitting them to the low-energy experimental data on the total cross sections of $\pi^+p \to K^+\Sigma^+(1385)$ reaction.

For the $pp \to nK^+\Sigma^+(1385)$ reaction, the full invariant scattering amplitude in our calculation is composed of two parts corresponding to the s-channel $\Delta^*(1940)$ resonance, and u-channel $\Lambda(1115)$ hyperon pole, which are produced by the π^+-meson exchanges,

$$\mathcal{M} = \sum_{i=s,\ u}\mathcal{M}_i. \quad (22)$$

Each of the above amplitudes can be obtained straightforwardly with the effective couplings and following the Feynman rules. Here we give explicitly the amplitude $\mathcal{M}_s$, as an example,

$$\begin{aligned} \mathcal{M}_s &= \frac{\sqrt{2}g_{\pi NN}g_{\pi N\Delta^*}}{m_\pi}F_\pi^{NN}(k_\pi^2)F_\pi^{\Delta^*N}(k_\pi^2)F_s(q^2_{\Delta^*})\times \\ &G_\pi(k_\pi^2)\bar{u}^\mu(p_4,s_4)(-\frac{g_1}{m_K}\not{p}_5 g_{\mu\rho} + \frac{g_2}{m_K^2}p_{5\mu}p_{5\rho})\times \\ &G^{\rho\sigma}_{\Delta^*}(q_s)k_{\pi\sigma}\gamma_5 u(p_1,s_1)\bar{u}(p_3,s_3)\gamma_5 u(p_2,s_2) \\ &+(\text{exchange term with } p_1 \leftrightarrow p_2), \end{aligned} \quad (23)$$

where s_i ($i = 1,2,3$) and p_i ($i = 1,2,3$) represent the spin projection and 4-momenta of the two initial protons and final neutron, respectively. While p_4 and p_5 are the 4-momenta of the final $\Sigma^+(1385)$ and K^+ meson, respectively. And s_4 stands for the spin projection of $\Sigma^+(1385)$. In Eq. (23), $k_\pi = p_2 - p_3$ and $q_{\Delta^*} = p_4 + p_5$ stand for the 4-momenta of the exchanged π^+ meson and intermediate $\Delta^*(1940)$ resonance. And $G_\pi(k_\pi^2)$ is the pion meson propagator,

$$G_\pi(k_\pi^2) = \frac{i}{k_\pi^2 - m_\pi^2}. \quad (24)$$

For $pp \to pK^+\Lambda(1520)$ reaction, we need also the relevant off-shell form factors for πNN and $\pi N\Delta^*$ vertexes, which have been already included in the amplitude of Eq. (23), and we take them as,

$$F_\pi^{NN}(k_\pi^2) = \frac{\Lambda_\pi^2 - m_\pi^2}{\Lambda_\pi^2 - k_\pi^2}, \quad (25)$$

$$F_\pi^{\Delta^*N}(k_\pi^2) = \frac{\Lambda_\pi^{*2} - m_\pi^2}{\Lambda_\pi^{*2} - k_\pi^2}, \quad (26)$$

with k_π the 4-momentum of the exchanged π meson. The cutoff parameters are taken as $\Lambda_\pi = \Lambda_\pi^* = 1.1$ GeV, with which the experimental data on $pp \to nK^+\Sigma^+(1385)$ reaction can be reproduced.

D. Cross sections for $\pi^+p \to K^+\Sigma^+(1385)$ reaction

The differential cross section for $\pi^+p \to K^+\Sigma^+(1385)$ reaction at center of mass (c.m.) frame can be expressed as

$$\frac{d\sigma}{d\cos\theta} = \frac{1}{32\pi s}\frac{|\vec{p}_3^{\,\text{c.m.}}|}{|\vec{p}_1^{\,\text{c.m.}}|}\left(\frac{1}{2}\sum_{s_{\Sigma^*},s_p}|T|^2\right), \quad (27)$$

where θ denotes the angle of the outgoing K^+ relative to beam direction in the c.m. frame, while $\vec{p}_1^{\,\text{c.m.}}$ and $\vec{p}_3^{\,\text{c.m.}}$ are the 3-momentum of the initial π^+ and final K^+ mesons. The total invariant scattering amplitude T is given by,

$$T = T_s + T_t + T_u\,. \quad (28)$$

From the amplitude, we can easily obtain the total cross sections of the $\pi^+p \to K^+\Sigma^+(1385)$ reaction as functions of the beam momentum p_{π^+}. By including all

the contributions from the s-channel Δ^* resonance, t-channel $K^{*0}(892)$, and u-channel $\Sigma^0(1193)$ and $\Lambda(1115)$ processes, at fixed cutoff parameters $\Lambda_s \neq \Lambda_t = \Lambda_u$, we perform four parameter (M_{Δ^*}, Γ_{Δ^*}, $\tilde{g}_1$, and $\tilde{g}_2$) χ^2-fit to the experimental data on total cross sections for $\pi^+p \to K^+\Sigma^+(1385)$ reaction. There is a total of 11 data points below $p_{\pi^+} = 4$ GeV.

By constraining the value of the cutoff parameters Λ_s and $\Lambda_t = \Lambda_u$ from 0.6 to 1.2 GeV, we get the minimal χ^2/dof 0.8 with $\Lambda_t = \Lambda_u = 0.6$ GeV and $\Lambda_s = 0.9$ GeV, and the fitted parameters are: $M_{\Delta^*} = 1940 \pm 24$ MeV, $\Gamma_{\Delta^*} = 172 \pm 94$ MeV, $\tilde{g}_1 = -0.36 \pm 0.19$, and $\tilde{g}_2 = 1.83 \pm 0.16$. The best fitting results for the total cross sections are shown in Fig. 3, comparing with the experimental data from Refs. [34–36]. The black-solid line represents the full results, while the contributions from the s-channel $\Delta^{++*}(1940)$ resonance, t-channel $K^{*0}(892)$ exchange, u-channel $\Lambda(1115)$ and $\Sigma^0(1193)$ terms are shown by the dash-dot-doted, dashed, dotted, and dash-doted lines, respectively. From Fig. 3, one can see that the description of the experimental data is quite well, especially, thanks to the contributions from the $\Delta^*(1940)$ resonance, the bump structure around $p_{\pi^+} = 1.8$ GeV can be described well. It is also show that the s-channel $\Delta^*(1940)$ resonance gives the dominant contribution, while the t-channel and u-channel diagrams give the minor contributions.

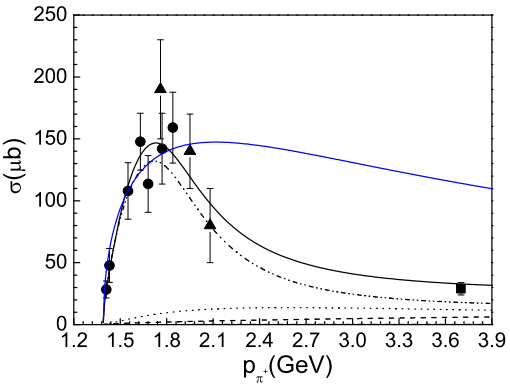

FIG. 3: (Color online) Total cross sections vs the beam momentum p_{π^+} for $\pi^+p \to K^+\Sigma^+(1385)$ reaction. The experimental data are taken from Ref. [34] (dots), Ref. [35] (triangles), and Ref. [36] (square). The curves are the contributions from s-channel $\Delta^*(1940)$ (dash-dot-dotted), t-channel K^{*0} (dashed), u-channel $\Sigma^0(1193)$ (dash-dotted) and $\Lambda(1115)$ (dotted), and the total contributions of them (black-solid), respectively. The blue-solid cure is obtained from the Stodolsky-Sakural model which will be discussed below.

In Fig. 4, the corresponding model predictions for the differential cross sections, $d\sigma/d\cos\theta$, of the $\pi^+p \to K^+\Sigma^+(1385)$ reaction are shown. Those results are obtained at $p_{\pi^+} = 1.42$ GeV [Fig. 4(a)], $p_{\pi^+} = 1.55$ GeV [Fig. 4(b)], $p_{\pi^+} = 1.62$ GeV [Fig. 4(c)], $p_{\pi^+} = 1.68$ GeV [Fig. 4(d)], $p_{\pi^+} = 1.77$ GeV [Fig. 4(e)], and $p_{\pi^+} = 1.84$ GeV [Fig. 4(f)], respectively. We also show the experimental data taken from Ref. [34] for comparison. One can see that by considering the dominant contributions from the $\Delta^*(1940)$, our model calculations can reasonably describe the angular distributions within the large experimental errors. However, at some energy points, such as $p_{\pi^+} = 1.55$ GeV [Fig. 4(b)], $p_{\pi^+} = 1.62$ GeV [Fig. 4(c)], and $p_{\pi^+} = 1.68$ GeV [Fig. 4(d)], our model calculations can not well reproduce the experimental measurements.

It is pointed out that the Stodolsky-Sakural model [37, 38] with dominant contribution from t-channel K^* exchange fits those production angular distributions reasonably well at all beam momenta [34] (see more details in Fig. 4 of that reference). The predictions of this model are that the form of the differential cross sections for $\pi^+p \to K^+\Sigma^+(1385)$ reaction is given by [34]

$$\frac{d\sigma}{d\cos\theta} \propto \frac{1-\cos^2\theta}{(t-M_{K^*}^2)^2}, \tag{29}$$

from where we can obtain the total cross sections [3] as shown in Fig. 3 by the blue-solid curve. One can see that the t-channel K^* exchange can reproduce well the experimental data from Ref. [34], but, it can not give the bump structure if we take those measurements of Refs. [35, 36] into account as shown in Fig. 3. Thus, the Stodolsky-Sakural model can reasonably describe the angular distribution at all momenta should not be surprising since the it considered only the experimental data from Ref. [34], where the bump structure does not appear because of the narrow energy range of measurements of Ref. [34].

On the other hand, we find that the experimental results of differential cross sections of Ref. [34] and the total cross sections data of Refs. [34–36] can not be simultaneously fitted well, which is because the differential cross sections data with large uncertainties are inconsistent between different angles and energies, hence, those data points about the differential cross sections from Ref. [34] are not taken into account in our best fit.

E. Partial decay widths of $\Delta^*(1940)$ resonance

With the Lagrangian densities of Eqs. (1) and (2), we can evaluated the $\Delta^*(1940)$ to $N\pi$ and $\Delta^*(1940)$ to

[3] We include also the phase space factor, $|\vec{p}_3^{\,\rm c.m.}|$, in our estimation. In this way the total cross section is obtained from $\sigma = N\int_{-1}^{1} \frac{1-\cos^2\theta}{(t-M_{K^*}^2)^2}|\vec{p}_3^{\,\rm c.m.}|d\cos\theta$, with a normalization $N = 1.54$ GeV.

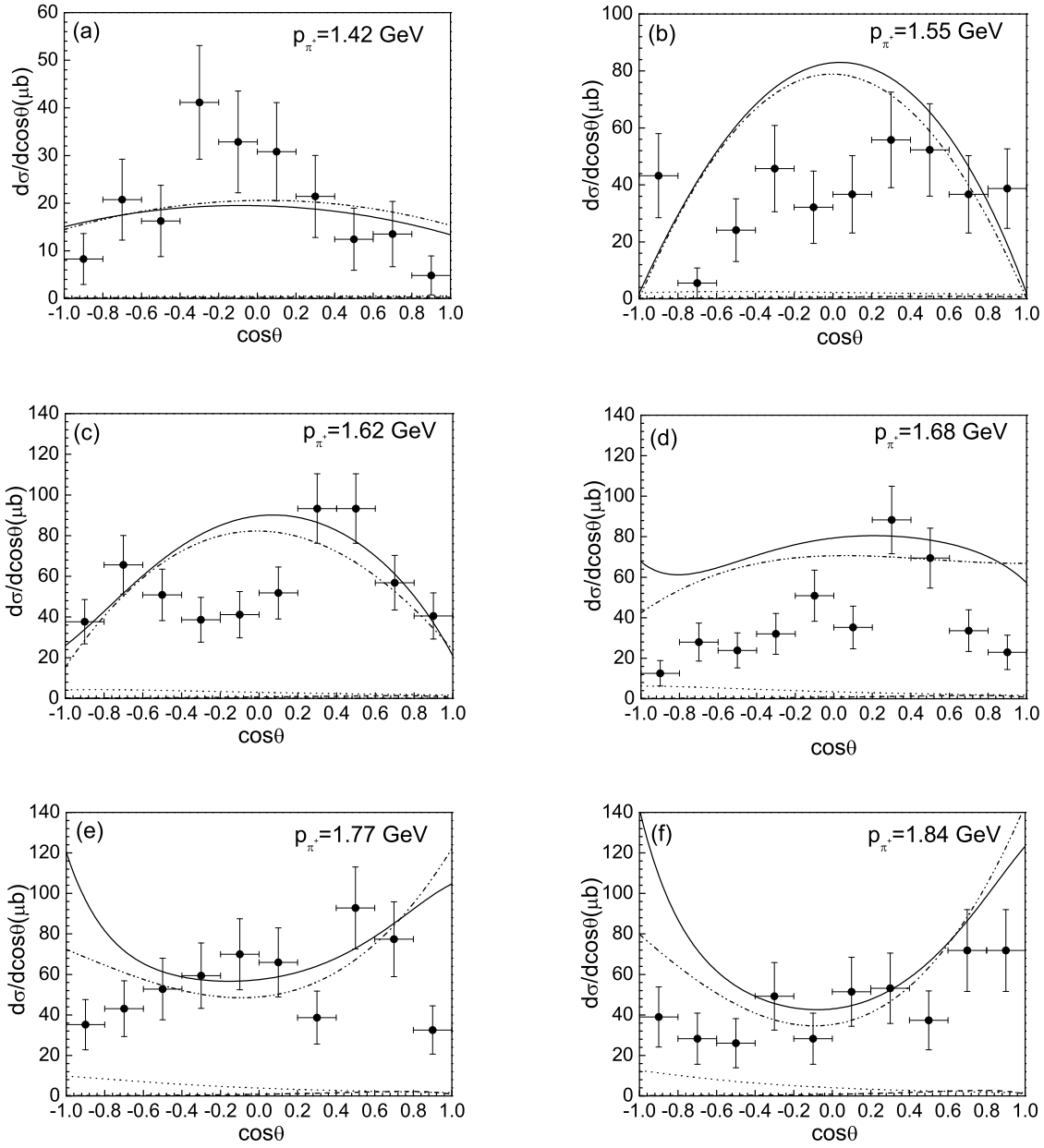

FIG. 4: Predictions of the differential cross sections, $d\sigma/d\cos\theta$, for $\pi^+ p \to K^+\Sigma^+(1385)$ reaction at different beam momentum. The experimental data are taken from Ref. [34]. The curves are the contributions from s-channel $\Delta^*(1940)$ (dash-dot-dotted), t-channel K^{*0} (dashed), u-channel $\Sigma^0(1193)$ (dash-dotted) and $\Lambda(1115)$ (dotted), and the total contributions of them (solid), respectively.

$\Sigma(1385)K$ partial decay widths,

$$\Gamma_{\Delta^*\to N\pi} = \frac{g^2_{\pi N\Delta^*}}{12\pi}\frac{|\vec{p}_N^{\,\rm c.m.}|^3}{m^2_\pi M_{\Delta^*}}(E_N - m_N), \quad (30)$$

$$\Gamma_{\Delta^*\to\Sigma^* K} = \frac{|\vec{p}_1^{\,\rm cm}|(E_{\Sigma^*}+M_{\Sigma^*})}{36\pi M_{\Delta^*}M^2_{\Sigma^*}}\Big\{\frac{2g_2^2M^2_{\Delta^*}}{m^4_K}|\vec{p}_1^{\,\rm cm}|^4 + \frac{2g_1g_2}{m^3_K}M_{\Delta^*}(M_{\Delta^*}-M_{\Sigma^*})(2E_{\Sigma^*}+M_{\Sigma^*})|\vec{p}_1^{\,\rm cm}|^2 + \frac{g_1^2}{m^2_K}(M_{\Delta^*}-M_{\Sigma^*})^2(2E^2_{\Sigma^*}+2E_{\Sigma^*}M_{\Sigma^*}+5M^2_{\Sigma^*})\Big\}, \quad (31)$$

where,

$$E_N = \frac{M^2_{\Delta^*}+m^2_N-m^2_\pi}{2M_{\Delta^*}}, \quad (32)$$

$$|\vec{p}_N^{\,\rm c.m.}| = \sqrt{E^2_N-m^2_N}, \quad (33)$$

$$E_{\Sigma^*} = \frac{M^2_{\Delta^*}+M^2_{\Sigma^*}-m^2_K}{2M_{\Delta^*}}, \quad (34)$$

$$|\vec{p}_1^{\,\rm cm}| = \sqrt{E^2_{\Sigma^*}-M^2_{\Sigma^*}}\,. \quad (35)$$

With the values of M_{Δ^*}, Γ_{Δ^*}, $\tilde{g}_1$ and $\tilde{g}_2$ obtained from the present fit, we get $\mathrm{Br}(\Delta^* \to N\pi)\times\mathrm{Br}(\Delta^* \to \Sigma^* K) = (0.52 \pm 0.13)\%$ with the error from the uncertainty of the fitted parameters.

On the other hand, the fitted results for the mass and total decay width of the $\Delta^*(1940)$ resonance are compatible with previous analysis in Ref. [39],

$$M_{\Delta^*(1940)} = 1940 \pm 100 \text{ MeV}, \quad (36)$$
$$\Gamma_{\Delta^*(1940)} = 200 \pm 100 \text{ MeV}, \quad (37)$$

quoted in PDG [2]. Next, by using the branch ratio of $\mathrm{Br}(\Delta^*(1940) \to N\pi)$ obtained in Ref. [39] and the total decay width of $\Gamma_{\Delta^*(1940)}$ from our present fit, we can determine the strong coupling constant, $g_{\pi N\Delta^*} = 0.35 \pm 0.12$ from the relation of Eq. (30). Then we can easily obtain the values of the strong $\Delta^*(1940)\Sigma(1385)K$ coupling constants g_1 and g_2,

$$g_1 = -1.04 \pm 0.38, \quad (38)$$
$$g_2 = 5.24 \pm 2.30. \quad (39)$$

Furthermore, the branch ration $\mathrm{Br}(\Delta^* \to \Sigma^* K)$ and partial decay width $\Gamma_{\Delta^* \to \Sigma^* K}$ are $(10.4 \pm 4.9)\%$ and 17.9 ± 12.9 MeV, respectively. We find that the $\Sigma^* K$ decay mode of the $\Delta^*(1940)$ resonance could be larger than the $N\pi$ channel, if one attributes the bump structure in the total cross sections of $\pi^+ p \to K^+\Sigma^+(1385)$ reaction [34–36], to the effects produced by this resonance, as implicitly assumed in this work. This large coupling of the two-star $D-$wave $J^P = 3/2^-$ $\Delta^*(1940)$ resonance to the $\Sigma^* K^+$ channel will confirm/get support from the QM results of Capstick, and Roberts in Ref. [18], as mentioned above.

III. NUMERICAL RESULTS FOR $pp \to nK^+\Sigma^+(1385)$ REACTION

With the formalism and ingredients given above, the calculations of the differential and total cross sections for $pp \to nK^+\Sigma^+(1385)$ are straightforward,

$$d\sigma(pp \to nK^+\Sigma^+(1385)) = \frac{1}{4}\frac{m_p^2}{F}\sum_{s_1,s_2}\sum_{s_3,s_4}|\mathcal{M}|^2 \times \frac{m_n d^3p_3}{E_3}\frac{m_{\Sigma^+(1385)}d^3p_4}{E_4}\frac{d^3p_5}{2E_5}\delta^4(p_1+p_2-p_3-p_4-p_5), \quad (40)$$

with the flux factor

$$F = (2\pi)^5\sqrt{(p_1\cdot p_2)^2 - m_p^4}\,. \quad (41)$$

The total cross section versus the beam energy ($\mathrm{p_{lab}}$) of the proton for the $pp \to nK^+\Sigma^+(1385)$ reaction is calculated by using a Monte Carlo multi-particle phase space integration program. The results for beam energies $\mathrm{p_{lab}}$ from just above the production threshold 3.2 GeV to 6.5 GeV are shown in Fig. 5. The dotted, and dash-dotted lines stand for contributions from $\Lambda(1115)$ and $\Delta^*(1940)$ resonance, respectively. Their total contributions are shown by the solid line. [4] From Fig. 5, we can see that the contribution from the $\Delta^*(1940)$ resonance is predominant in the whole considered energy region. For comparison, we also show the experimental data [13, 14] in Fig. 5, from where we can see that our predictions for the total cross sections of $pp \to nK^+\Sigma^+(1385)$ reaction are in agreement with the experimental measurements.

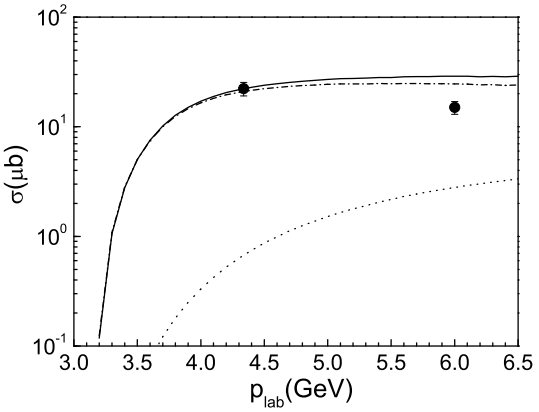

FIG. 5: Total cross sections vs beam energy $\mathrm{p_{lab}}$ of proton for the $pp \to nK^+\Sigma^+(1385)$ reaction from present calculation. The dotted and dash-dotted lines stand for contributions from $\Lambda(1115)$ pole and $\Delta^*(1940)$ resonance, respectively. Their total contribution are shown by the solid line. The experimental data are taken from Refs. [13, 14].

In addition to the total cross sections, we also compute the differential distributions for $pp \to nK^+\Sigma^+(1385)$ reaction, namely the angular distributions of all final-state particles in the overall center-of-mass frame (CMS), as well as distributions in both the Gottfried-Jackson and helicity frames as introduced in Refs. [14, 40]. Like Dalitz plots, the helicity angle distributions provide insight into the three-body final state. While the information contained in the Gottfried-Jackson angle distributions is complementary to that of a Dalitz plot, as this angular distribution can give insight into the scattering process, especially concerning the involved partial waves.

The corresponding theoretical results are shown in Fig. 6 with the experimental data taken from Ref. [14], where the dashed lines are pure phase space distributions,

[4] Since the t-channel K^{*0} meson and u-channel $\Sigma^0(1193)$ exchange give very small contribution to the $\pi^+ p \to K^+\Sigma^+(1385)$ reaction, especially for the invariant mass of $K\Sigma(1385)$ around 2 GeV, we ignore these contributions in the calculation for the $pp \to nK^+\Sigma^+(1385)$ reaction.

while the solid lines are full results from our model. We can see that our theoretical results with the dominant contributions from the $\Delta^*(1940)$ resonance can describe the experimental data fairly well, and only the phase space is far from the data. The agreement of our model calculation with the experimental data in Fig. 6 indicates that the HADES data support the important role played by an odd-parity $3/2^-$ $\Delta^*(1940)$ resonance with a mass in the region of 1940 MeV and a width of around 200 MeV.

In Fig. 6 (a), (b), and (c), we show the $\Sigma^+(1385)$, neutron and K^+ angular distributions in the CMS, respectively. The anisotropy of the experimental distributions can be well reproduced thanks to the contributions from the $\Delta^*(1940)$ resonance. The results obtained in the helicity frame with respect to the angle, Θ^{a-b}_{c-d}, which represents the angel between particles "a" and "b" in the "c" and "d" reference frame (see more details in Ref. [14]), are shown in Fig. 6 (d), (e), and (f), while Fig. 6 (g), (h), and (i) depict the distributions of the Gottfried-Jackson angles.

Furthermore, the corresponding momentum distribution [5] of the $\Sigma^+(1385)$ and K^+ meson, the $K\Sigma(1385)$ invariant mass spectrum, and also the Dalitz Plot for the $pp \to nK^+\Sigma^+(1385)$ reaction at beam momentum $\mathrm{p_{lab}} = 4.34$ GeV (corresponding to kinetic beam energy $\mathrm{T_p} = 3.5$ GeV[6]), which is accessible for HADES Collaboration [14], are calculated and shown in Fig. 7(a), Fig. 7(b), Fig. 7(c), and Fig. 7(d), respectively. The dashed lines are pure phase space distributions, while, the solid lines are full results from our model. From Fig. 7(c), we can see that at $\mathrm{p_{lab}} = 4.34$ GeV, our model results on the the momentum distribution of the $\Sigma^+(1385)$ are much different with the phase space. On the other hand, there is a clear bump in the $K\Sigma(1385)$ invariant mass distribution, which is produced by including the contribution from $\Delta^*(1940)$ resonance.

The momentum distribution, invariant mass spectra and the Dalitz plots in Fig. 7 show direct information about the $pp \to nK^+\Sigma^+(1385)$ reaction mechanism and may be tested by the future experiments.

In summary, owing to the important role played by the resonant contribution in the $pp \to nK^+\Sigma^+(1385)$ reaction, our model can describe the experimental data of the angle distributions well, which indicate that recent HADES data support the existence of this $\Delta^*(1940)$ resonance, and more accurate data for this reaction can be used to improve our knowledge on the $\Delta^*(1940)$ properties, which are at present poorly known. Our present calculation offers some important clues for the mechanisms of the $\pi^+p \to K^+\Sigma^+(1385)$ and $pp \to nK^+\Sigma^+(1385)$ reactions and makes a first effort to study the role of the $\Delta^*(1940)$ resonance in relevant reactions.

[5] It is noteworthy that our results are calculated in the reaction laboratory frame, in which the target proton is at rest.

[6] $\mathrm{p_{lab}} = \sqrt{\mathrm{E_{lab}}^2 - m_p^2} = \sqrt{(\mathrm{T_p} + m_p)^2 - m_p^2}$.

IV. SUMMARY

In this paper, the $\Sigma^+(1385)$ hadronic production in proton-proton and π^+p collisions are studied within the combination of the effective Lagrangian approach and the isobar model. For $\pi^+p \to K^+\Sigma^+(1385)$ reaction, in addition to the "background" contributions from t-channel $K^{*0}(892)$ exchange, u-channel $\Sigma^0(1193)$ and $\Lambda(1115)$ exchange, we also considered the contribution from the $\Delta^*(1940)$ resonance in the s-channel, which has significant coupling to $K\Sigma(1385)$ channel. We show that the inclusion of the $\Delta^*(1940)$ resonance leads to a fairly good description of the low energy experimental total cross section data of $\pi^+p \to K^+\Sigma^+(1385)$ reaction. The s-channel $\Delta^*(1940)$ resonance gives the dominant contribution, while the t-channel and u-channel diagrams give the minor contributions.

From χ^2-fit to the available experimental data for the $\pi^+p \to K^+\Sigma(1385)$ reaction, we get the mass and total decay width of $\Delta^*(1940)$, which are $M_{\Delta^*} = 1940 \pm 24$ MeV and $\Gamma_{\Delta^*} = 172 \pm 94$ MeV, respectively. With the value 0.35 ± 0.11 for the $\Delta^*(1940)N\pi$ coupling constant $g_{\pi N\Delta^*}$, which is obtained with the branching ration $\mathrm{Br}(\Delta^*(1940) \to N\pi) = (5 \pm 2)\%$, we determine the strong couplings $g_{1,2}$ for the $\Delta^*(1940)K\Sigma(1385)$ vertex as $g_1 = -1.04 \pm 0.38$ and $g_2 = 5.24 \pm 2.30$. With these above values, we have calculated the partial decay width of $\Delta^*(1940) \to \Sigma(1385)K$, and we obtain $\Gamma_{\Delta^* \to \Sigma^* K} = 17.9 \pm 12.9$ MeV and $\mathrm{Br}(\Delta^* \to \Sigma^* K) = (10.4 \pm 4.9)\%$. It is shown that the $\Delta^*(1940)$ resonance would have a large decay width into $\Sigma(1385)K$, which will be compatible with the findings of the QM approach of Ref. [18].

Based on the study of $\pi^+p \to nK^+\Sigma^+(1385)$ reaction, we study the $pp \to nK^+\Sigma^+(1385)$ reaction with the assumption that the production mechanism is due to the π^+-meson exchanges. We give our predictions about total cross sections for the $pp \to nK^+\Sigma^+(1385)$ reaction. We find that our theoretical results with the dominant contributions from the $\Delta^*(1940)$ resonance can describe fairly well the experimental data both on total cross sections and differential cross sections. Thus, the HADES data support the important role played by the $\Delta^*(1940)$ resonance with a mass in the region of 1940 MeV and a width of around 200 MeV. Furthermore, we also demonstrate that the invariant mass distribution and the Dalitz Plot provide direct information of the $pp \to nK^+\Sigma^+(1385)$ reaction mechanisms and may be tested by the future experiments.

Finally, we would like to stress that the $pp \to nK^+\Sigma^+(1385)$ reaction is a new excellent source for studying Δ^* resonances. And due to the important role played by the $\Delta^*(1940)$ resonance in the $\pi^+p \to K^+\Sigma^+(1385)$ and $pp \to nK^+\Sigma^+(1385)$ reactions, accurate data for these reactions can be used to improve

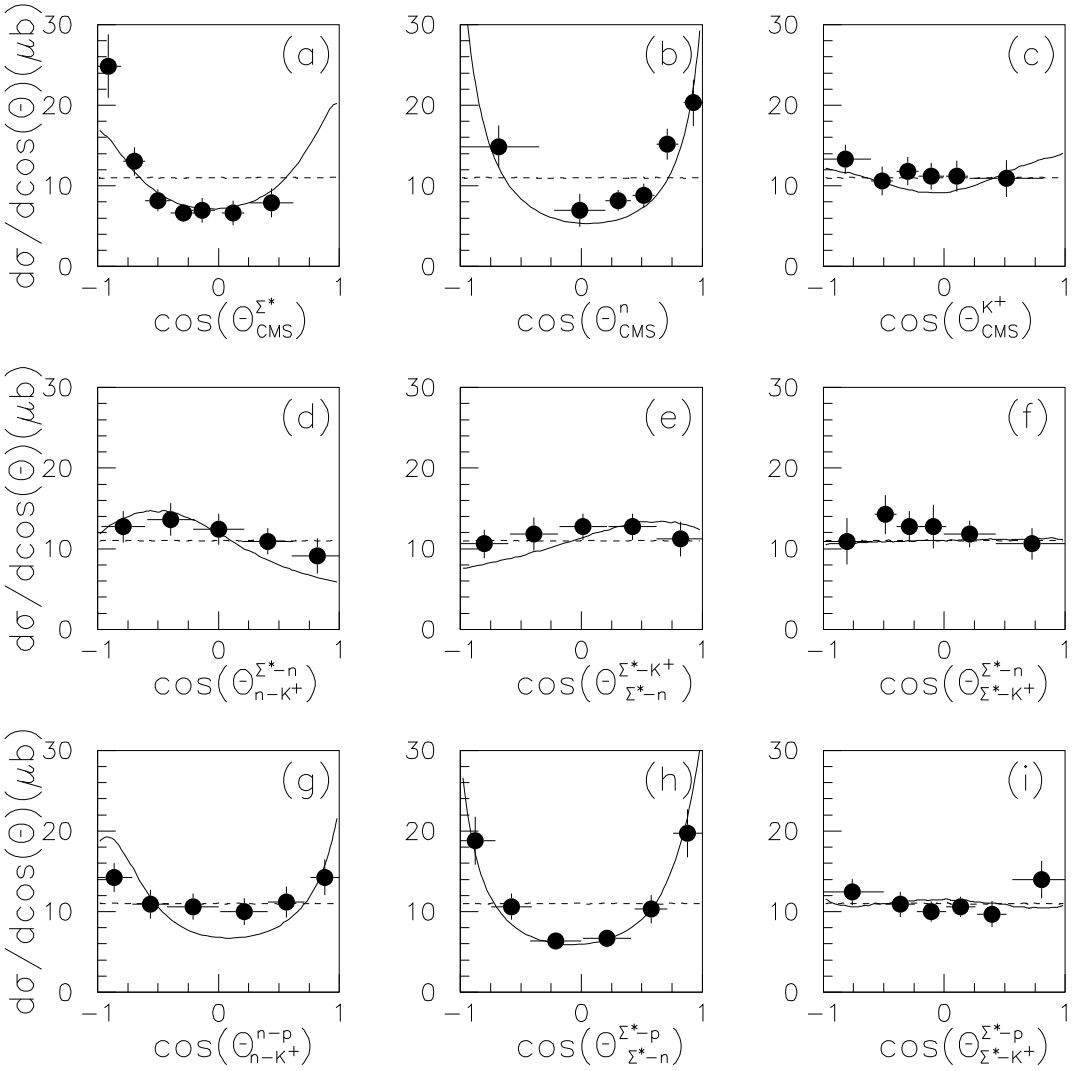

FIG. 6: Angular differential cross sections for the $pp \to nK^+\Sigma^+(1385)$ reaction in CMS [(a): $\Theta^{\Sigma^*}_{\rm CMS}$, (b): $\Theta^{n}_{\rm CMS}$, (c): $\Theta^{K^+}_{\rm CMS}$], helicity [(d): $\Theta^{\Sigma^*-n}_{n-K^+}$, (e): $\Theta^{\Sigma^*-K^+}_{\Sigma^*-n}$, (f): $\Theta^{\Sigma^*-n}_{\Sigma^*-K^+}$], and Gottfried-Jackson [(g): $\Theta^{n-p}_{n-K^+}$, (h): $\Theta^{\Sigma^*-p}_{\Sigma^*-n}$, (i): $\Theta^{\Sigma^*-p}_{\Sigma^*-K^+}$] reference frames. The dashed lines are pure phase space distributions, while the solid lines are full results from our model. The experimental data are taken from Ref. [14].

our knowledge on the $\Delta^*(1940)$ properties, which are at present poorly known.

Acknowledgments

We would like to thank Juan Nieves, Bo-Chao Liu and Xu Cao for useful discussions. This work is partly supported by DGI and FEDER funds, under contract No. FIS2011-28853-C02-01 and FIS2011-28853-C02-02, the Spanish Ingenio-Consolider 2010 Program CPAN (CSD2007-00042), Generalitat Valenciana under contract PROMETEO/2009/0090 and by the National Natural Science Foundation of China under grants 11105126, 11035006, 11121092, 11261130311 (CRC110 by DFG and NSFC), the Chinese Academy of Sciences under Project No. KJCX2-EW-N01 and the Ministry of Science and Technology of China (2009CB825200). We acknowledge the support of the European Community-Research Infrastructure Integrating Activity "Study of Strongly Interacting Matter" (HadronPhysics3, Grant Agreement No. 283286) under the Seventh Framework Programme of EU.

[1] E. Klempt and J. M. Richard, Rev. Mod. Phys. **82**, 1095 (2010).

[2] J. Beringer et al., [Particel Data Group], Phys. Rev. D

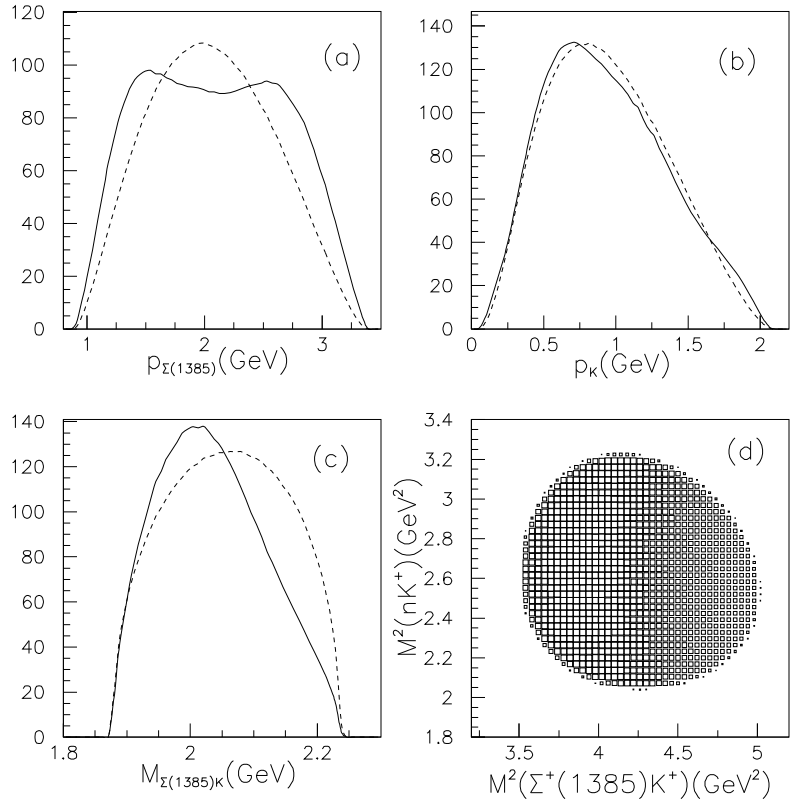

FIG. 7: Momentum distribution (arbitrary units), invariant mass spectrum (arbitrary units), and Dalitz Plot for the $pp \to nK^+\Sigma^+(1385)$ reaction at beam energy $p_{lab} = 4.34$ GeV comparing with the phase space distribution.The dashed lines are pure phase space distributions, while the solid lines are full results from our model.

86, 010001 (2012).

[3] S. Capstick and W. Robert, Prog. Part. Nucl. Phys. **45**, S241 (2000), and references therein.

[4] D. Gamermann, C. Garcia-Recio, J. Nieves and L. L. Salcedo, Phys. Rev. D **84**, 056017 (2011).

[5] S. Sarkar, B. -X. Sun, E. Oset and M. J. Vicente Vacas, Eur. Phys. J. A **44**, 431 (2010).

[6] E. Oset and A. Ramos, Eur. Phys. J. A **44**, 445 (2010).

[7] B. -X. Sun, H. -X. Chen and E. Oset, Eur. Phys. J. A **47**, 127 (2011).

[8] J. -J. Xie and B. -S. Zou, Phys. Lett. B **649**, 405 (2007).

[9] M. Doring, C. Hanhart, F. Huang, S. Krewald, U. -G. Meissner and D. Ronchen, Nucl. Phys. A **851**, 58 (2011).

[10] A. Zhang, Y. R. Liu, P. Z. Huang, W. Z. Deng, X. L. Chen and S. -L. Zhu, High Energy Phys. Nucl. Phys. **29**, 250 (2005).

[11] J. -J. Wu, S. Dulat and B. S. Zou, Phys. Rev. D **80**, 017503 (2009).

[12] J. -J. Wu, S. Dulat and B. S. Zou, Phys. Rev. C **81**, 045210 (2010).

[13] S. Klein, W. Chinowsky, R. R. Kinsey, M. Mandelkern, J. Schultz and T. H. Tan, Phys. Rev. D **1**, 3019 (1970).

[14] G. Agakishiev *et al.* [HADES Collaboration], Phys. Rev. C **85**, 035203 (2012).

[15] E. Ferrari, Phys. Rev. **175**, 2003 (1968).

[16] W. Chinowsky, R. R. Kinsey, S. L. Klein, M. Mandelkern, J. Schultz, F. Martin, M. L. Perl and T. H. Tan, Phys. Rev. **165**, 1466 (1968).

[17] S. Capstick, Phys. Rev. D **46**, 2864 (1992).

[18] S. Capstick, and W. Roberts, Phys. Rev. D **58**, 074011 (1998).

[19] Y. Oh, C. M. Ko and K. Nakayama, Phys. Rev. C **77**, 045204 (2008).

[20] P. Gao, J. -J. Wu and B. S. Zou, Phys. Rev. C **81**, 055203 (2010).

[21] Y. -H. Chen and B. -S. Zou, Phys. Rev. C **88**, 024304 (2013).

[22] J. He, arXiv:1311.0571 [nucl-th].

[23] J. -J. Xie, A. Martinez Torres, E. Oset and P. Gonzalez, Phys. Rev. C **83**, 055204 (2011).

[24] H. Kamano, B. Julia-Diaz, T. -S. H. Lee, A. Matsuyama and T. Sato, Phys. Rev. C **80**, 065203 (2009).

[25] N. Suzuki, B. Julia-Diaz, H. Kamano, T. -S. H. Lee, A. Matsuyama and T. Sato, Phys. Rev. Lett. **104**, 042302 (2010).

[26] H. Kamano, B. Julia-Diaz, T. -S. H. Lee, A. Matsuyama and T. Sato, Phys. Rev. C **79**, 025206 (2009).

[27] H. Kamano, S. X. Nakamura, T. S. H. Lee and T. Sato, Phys. Rev. D **84**, 114019 (2011).

[28] A. Martinez Torres, K. P. Khemchandani, U. -G. Meissner and E. Oset, Eur. Phys. J. A **41**, 361 (2009).

[29] A. Martinez Torres, K. P. Khemchandani and E. Oset, Phys. Rev. C **79**, 065207 (2009)

[30] B. S. Zou and F. Hussain, Phys. Rev. C **67**, 015204 (2003).

[31] S. -H. Kim, S. -I. Nam, A. Hosaka and H. -C. Kim, Phys. Rev. D **88**, 054012 (2013).
[32] J. -J. Xie, B. -C. Liu and C. -S. An, Phys. Rev. C **88**, 015203 (2013).
[33] J. -J. Xie and B. -C. Liu, Phys. Rev. C **87**, 045210 (2013).
[34] P. Hanson, G. E. Kalmus and J. Louie, Phys. Rev. D **4**, 1296 (1971); see also http://hepdata.cedar.ac.uk/view/ins74874.
[35] S. Dagan, Z. Ming Ma, J. W. Chapman, L. R. Fortney, and E. C. Fowler, Phys. Rev. **161**, 1384 (1967).
[36] W. R. Butler, D. G. Coyne, G. Goldhaber, J. Macnaughton and G. H. Trilling, Phys. Rev. D **7**, 3177 (1973).
[37] L. Stodolsky and J. J. Sakurai, Phys. Rev. Lett. **11**, 90 (1963).
[38] L. Stodolsky, Phys. Rev. **134**, B1099 (1964).
[39] R. E. Cutkosky, C. P. Forsyth, J. B. Babcock, R. L. Kelly and R. E. Hendrick, COO-3066-157. *Baryon* 80 Proceedings of the 4th International Conference on Baryon Resonances, Toronto, Canada, July 14-16, 1980, ed. N. Isgur, University of Toronto, 1981, p.19.
[40] M. Abdel-Bary *et al.* [COSY-TOF Collaboration], Eur. Phys. J. A **46**, 27 (2010); [Erratum-ibid. A **46**, 435 (2010)].